Engineering Structures 292 (2023) 116531

Contents lists available at ScienceDirect

Engineering Structures

journal homepage: www.elsevier.com/locate/engstruct

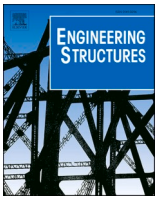

Experimental investigation on the shear behaviour of the brickwork-backfill interface in masonry arch bridges

Bowen Liu [a], Anastasios Drougkas [b], Vasilis Sarhosis [a,*], Colin C. Smith [c], Matthew Gilbert [c]

[a] School of Civil Engineering, University of Leeds, Leeds LS2 9JT, UK
[b] Serra Húnter Fellow, Department of Strength of Materials and Structural Engineering, Universitat Politècnica de Catalunya (UPC-BarcelonaTech), C/Colom 11, 08222 Terrassa, Spain
[c] Department of Civil and Structural Engineering, University of Sheffield, Sheffield S1 3JD, UK

ARTICLE INFO

Keywords:
Brickwork-backfill interfaces
Backfill
Bond type
Interface friction angle
Masonry arch bridges

ABSTRACT

This paper presents the results from an experimental campaign to characterise the shear behaviour of the brickwork-backfill interaction in masonry arch bridges. Two representative backfill materials found in real masonry arch bridges (compacted crushed limestone and clay) were sheared against brickwork masonry specimens with two different bond patterns (a soldier course bond and an English bond). The results demonstrated that the interface shear behaviour between masonry and backfill was different from the internal shear behaviour of backfill materials. When compacted crushed limestone was adopted as the backfill material, the ratio between the masonry-limestone interface friction angle (φ_i) and the internal friction angle (φ) of limestone was determined to lie within the range from 0.70 to 0.75. However, when clay was used as backfill material, the φ_i/φ ratio was much lower, and of the order of 0.51 to 0.52 under the assumption of zero-cohesion at the interface, or 0.35 to 0.39 if interface cohesion was considered. Moreover, the properties of the backfill material had a significant influence on the interface shear behaviour, whereas the effects of brickwork bonding pattern were marginal. This study provides valuable insight into the identification of brickwork-backfill interface parameters for the numerical analysis of masonry arch bridges.

1. Introduction

Masonry arch bridges form a vital part of the transportation infrastructure systems of many countries. For example, it is estimated that there are approximately 40,000 masonry arch bridges in the UK [1]. To assess load-bearing capacity and to predict the in-service behaviour of masonry arch bridges, reliable numerical or analytical methods are needed. A number of input parameters are generally required for these methods to characterize the behaviour of bridges, including the material properties of the masonry units, mortar joints and backfill, as well as the interface parameters between masonry and backfill. The selection of these parameters plays a determining role in whether the numerical or analytical methods employed can accurately model structural performance, and varying these parameters can significantly impact the calculation results [2,3]. The masonry material properties can be determined by standard small-scale laboratory experiments [4,5]. Also, the properties of the backfill materials, including internal friction angle φ and cohesion c, can be characterised via direct shear box tests [6]. However, although masonry and backfill interface parameters (i.e., interface friction angle φ_i (or friction coefficient μ_i), interface cohesion c_i and stiffness) have been recognised as having a strong influence on the load-carrying capacity of masonry arch bridges [7], there is no commonly used experimental procedure for obtaining them.

Table 1 lists soil properties and interface parameters for masonry arch bridges adopted by researchers in recent studies. A noticeable discrepancy can be observed in the selection of these parameters across studies. For instance, most researchers adopted a ratio of the friction angle of the interface between the masonry-backfill and of the backfill itself (φ_i/φ) at approximately 0.70, with a minimum of 0.46 and a maximum of 0.82. One of the reasons for these discrepancies may be the different backfill materials investigated. However, even the studies that adopted the same backfill material (e.g., both [8;9] used crushed limestone backfill), they assigned different ratios of φ_i/φ in their numerical models. This inconsistency in parameter settings can be primarily attributed to the limited understanding of the interface interaction between masonry and backfill materials. Moreover, to the best of the

* Corresponding author at: Vasilis Sarhosis, School of Civil Engineering, University of Leeds, Leeds LS2 9JT, UK.
E-mail address: V.sarhosis@leeds.ac.uk (V. Sarhosis).

https://doi.org/10.1016/j.engstruct.2023.116531
Received 26 January 2023; Received in revised form 20 May 2023; Accepted 24 June 2023
Available online 28 June 2023

authors' knowledge, no study has considered the influence of backfill properties or masonry bond patterns when selecting interface parameters, despite the fact that masonry of different bond patterns has different surface roughness and texture, which may lead to variations in interface frictional parameters, as previously reported [10].

In the past, direct shear box tests were widely used to evaluate the shear behaviour of a variety of soils and interfaces between soil and construction materials (i.e., wood, steel and concrete) [18–20]. For instance, for a cohesionless sand material, as the sand particles become more angular, the 'interlocking' between particles becomes more pronounced, leading to higher shear strength and internal friction angle [21]. Also, the roughness and texture of the surface, soil properties, particle size, and moisture content have been identified to be the most critical factors affecting the shear behaviour between soil and construction materials [22–26]. Moreover, previous research has pointed out that the peak shear stress at soil-structure interfaces is most likely to be different from the shear strength of the soil itself, depending on the relative surface roughness. As the surface roughness increases, the shear strength of the interface tends to increase and gradually approaches that of e.g., sand when the surface roughness is close to the particle size [27]. However, for clay-structure interfaces, except in the case of very smooth surfaces, the interface shear strength is often assumed to be approximately equal to, or slightly smaller than, the shear strength of the clay itself [25,28]. Together these studies emphasize that the shear behaviour of the soil-structure interface largely depends on the soil properties and structure surface characteristics.

In the case of masonry arch bridges, the backfill is responsible for transmitting and distributing live loads from the road or rail surface to the arch barrel and for laterally stabilising the arch barrel as it sways under loading. Therefore, understanding the shear behaviour between masonry and backfill materials is essential in assessing the mechanical behaviour of masonry arch bridges. Moreover, experimental evidence is necessary to establish reasonable friction parameters at the masonry-backfill interface when developing numerical models of masonry arch bridges.

To this end, this paper aims to present an experimental procedure to characterise the shear behaviour of the backfill-arch ring and backfill-spandrel wall interaction in masonry arch bridges. A total of 36 experimental tests have therefore been carried out to characterise the frictional properties of limestone and clay, as well as the interface frictional parameters of the four types of brickwork-backfill interfaces typically found in masonry arch bridges in the field. Based on the test results and post-shear failure characterisations, the influence of masonry bond patterns and backfill properties on the interface shear behaviour was analysed. Finally, the ratios of friction angle between the backfill and brickwork-backfill interfaces were summarised according to the types of backfill and the cohesion characteristics of brickwork-backfill interfaces.

2. Experimental programme

2.1. Units, mortar, and masonry specimens

High compressive strength/low water absorption fired clay bricks (hereafter referred to as Type A bricks) were used in the study as masonry units. The bricks had nominal dimensions of 215 mm length × 102 mm width × 63 mm height and a density of 2,470 kg/m^3. The compressive strength, Young's modulus, flexural strength, and also the tensile strength of the Type A bricks were characterised via standard compression tests, three-point bending tests, and Brazilian (splitting) tests, following the procedure and requirements outlined in [29,30]. Table 2 lists the number of test samples, the determined strength properties, and also the coefficient of variation (CV) of the test results for the Type A bricks used. Cement mortar with a mix ratio of 1:2 (cement/sand by volume) and a water/binder ratio of 0.4 (by weight) was selected as the bonding material to ensure good joint durability and rapid hardening time.

Previous studies have pointed out that the hardness of construction materials can affect the shear strength parameters at soil-construction material interfaces, particularly for soft construction materials such as wood, geomembranes, and soft polymer [31–33]. When relatively high normal stresses are applied, the motion of soil particles along the soil-solid contact interface is characterised by both sliding and ploughing, resulting in an increase in interface friction [34,35]. However, this effect is observed to be less significant as the hardness of the construction material increases. For hard construction materials such as concrete and steel, the roughness and texture of the solid surface and soil characteristics, such as soil density, water content, particle size and morphology, are the dominating factors affecting interface behaviour [24,36], rather than the strength of the construction materials. The critical factor that determines whether a construction material is classified as 'soft' or 'hard' in shear box testing is whether the material's surface is disturbed by soil particles during shearing. In the study, the high strength bricks and cement mortar were used to achieve high durability of the brickwork specimens, avoiding damage to mortar joints by backfill particles during the tests, and maintaining the same surface roughness and texture over the twelve tests performed on each brickwork specimen. Moreover, according to the findings from the steel-soil interface and the concrete-soil interface tests, the strength properties of the bricks and mortar joints are not expected to affect the friction behaviour of the

Table 2
Material properties of bricks.

Material properties	Number of samples	Mean values (MPa)	CV
Compressive strength	9	111.3	6.2%
Flexural strength	8	19.8	9.6%
Tensile strength	9	6.7	13.5%
Young's modulus	9	31762.6	15.7%

Table 1
Frictional properties of backfill materials and masonry-backfill interface adopted in the previous numerical studies.

Studies	Types of backfill	Backfill properties		Masonry-backfill interface parameters		φ_i/φ
		Internal friction angle $\varphi(^\circ)$	Cohesion c(kPa)	Interface friction angle $\varphi_i(^\circ)$	Cohesion c_i(kPa)	
Sarhosis et al. 2019 [11]	Reddish-brown sand with a little clay	37	7	25	0	0.68
Gilbert et al. 2010 [8]	Crushed limestone	54.5	3.3	24.8	1.1	0.46
Grosman et al. 2021 [9]	50 mm graded crushed limestone	43.8	1	28	19	0.64
Forgács et al. 2021 [12]	Typical limestone	37	5	20	–	0.54
Scozzese et al. 2019 [13]	A granular mixture fill	38	–	31	–	0.82
Oliveira et al. 2010 [14]	Not specified	30	–	20	–	0.67
Pulatsu et al. 2019 [7]	Not specified	30	20	20	0	0.67
Bayraktar et al. 2021a [15]	Not specified	35	50	17	–	0.49
Bayraktar et al. 2021b [16]	Not specified	30	80	17	–	0.57
Pantò et al. 2022 [17]	Not specified	43.5	1	31	2.9	0.71

brickwork-backfill interface, as long as the brickwork surface is not disturbed.

2.2. Brickwork specimens

Given the fact that the roughness and texture of a solid surface can significantly affect the shear behaviour at soil-structure interfaces, two types of joint layouts were considered in the study to investigate the influence of bond patterns and joint arrangements on the shear behaviour at the masonry-backfill interface. In designing the brickwork specimens, a primary consideration was to employ bond patterns representative of those found in real brickwork masonry arch bridges. Fig. 1 shows a schematic drawing of a typical brickwork masonry arch bridge found in the UK. As shown in Fig. 1, the backfill material fills the void between the spandrel walls and arch barrel, and forms a level surface for vehicles and trains to pass over. Consequently, there are two types of masonry-backfill interfaces, namely spandrel wall-backfill interfaces and arch ring-backfill interfaces; see Fig. 1.

The primary function of spandrel walls in a masonry arch bridge is to resist the horizontal soil pressure from the backfill. Spandrel walls can be built in multi-wythe arrangements to provide better resistance to lateral soil pressures. For masonry arch bridges found in the UK, English bond and Flemish bond are the most widely used [37,38]. Compared to masonry constructed using Flemish bond, English bond has a lower mortar volume and higher strength, and is therefore more widely used in the construction of load-bearing components, including spandrel walls in brick-masonry bridges [39]. In this study, one of the two brickwork specimens was therefore designed to have the same layout of joints as English bond, to simulate the interaction between backfill and spandrel walls (Fig. 2 (a)). Brickwork with English bond is constructed by laying alternate courses of stretchers and headers. Joints between the stretchers were centred on the headers in the course below.

The main load-carrying element in a masonry arch bridge is the arch barrel, which may consist of a single ring or multiple concentric rings (multi-ring). Geometric parameters of an arch barrel (i.e., span-rise ratio, ring thickness) can significantly affect its load-carrying capacity. In addition, the spatial arrangement of bricks with mortar joints influences crack propagation and the mode of failure of the arch [9]. To simulate the joint arrangement on the extrados of an arch barrel, an aligned joint layout was adopted in this study as a second bond pattern [40]. More specifically, for a single-ring voussoir arch, bricks were laid directly at the side of one another along the arch line, with the narrow edge facing out. All joints were aligned when observed from the top of the arch (Fig. 1), which can be referred to as a soldier course bond type (Fig. 2 (b)).

Fig. 2 shows the method of constructing experimental specimens from brickwork with an English and a soldier course bond pattern. Both brickwork specimens had similar dimensions, measuring approximately 282 mm in length, 282 mm in width, and 102 mm in depth (single Wythe), allowing them to be accommodated by the shear box. To achieve the designed bond patterns within the confined space, Type A bricks were cut into four different sizes. More specifically, the brickwork specimen with an English bond pattern consisted of four bricks in size A, two each of bricks in sizes B, C, and D, while the specimen with a soldier course bond pattern contained six bricks in size A and four bricks in size B. The bricks were bonded with cement mortar joints measuring 10 mm in thickness. A 10 mm thickness was selected based on its common application in practice and its widespread adoption in experimental and numerical studies [41–44]. The brickwork joints were concave (see Fig. 3), which is representative of joint profiles found in real masonry arch bridges [45]. This concave shape had an approximate radius of 5 mm and a maximum depth of 4 mm, which was created by pressing a curved steel jointer against the joints before the mortar hardened. Moreover, the smeared mortar was removed from the surface of the brickwork specimens using a Nylon brush. The two specimens used in this study were constructed on the same day by the same experienced mason to minimize any variability in specimens.

2.3. Direct shear tests on backfill materials

The selection of soil is crucial, as its properties can considerably affect soil-structure interface behaviour. Typically, material that was easily accessible at the worksite was employed as backfill in the construction of masonry arch bridges, which means there is significant variation in backfill properties across bridges [46]. Although there is no comprehensive report on the materials most commonly used, available literature suggests that over 65% of masonry arch bridges have used clay, sand, and limestone gravel as the backfill material [47]. In addition, most previous experimental studies on masonry arch bridges have used clay and compacted crushed limestone as backfill materials [48,49]. Therefore, this study adopted these two widely used materials, i.e., compacted crushed limestone and cohesive puddling clay (also often called ‘puddle clay’), to assess the effects of soil properties on the shear behaviour of masonry-backfill interfaces.

Limestone is a cohesionless course-grained angular fill material. The grain-size distribution of the limestone used in this study is shown in

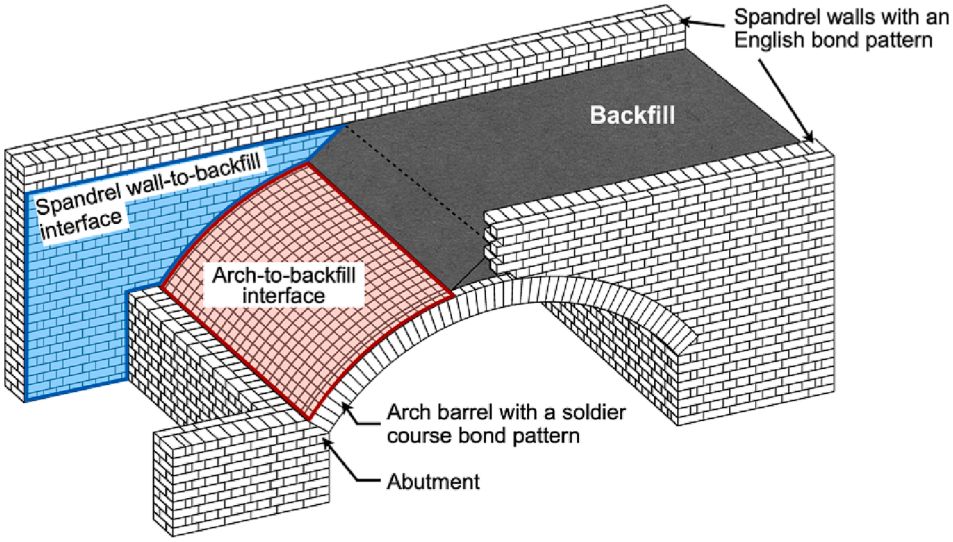

Fig. 1. Typical brickwork masonry arch bridge showing the spandrel wall-backfill interface and arch-backfill interfaces.

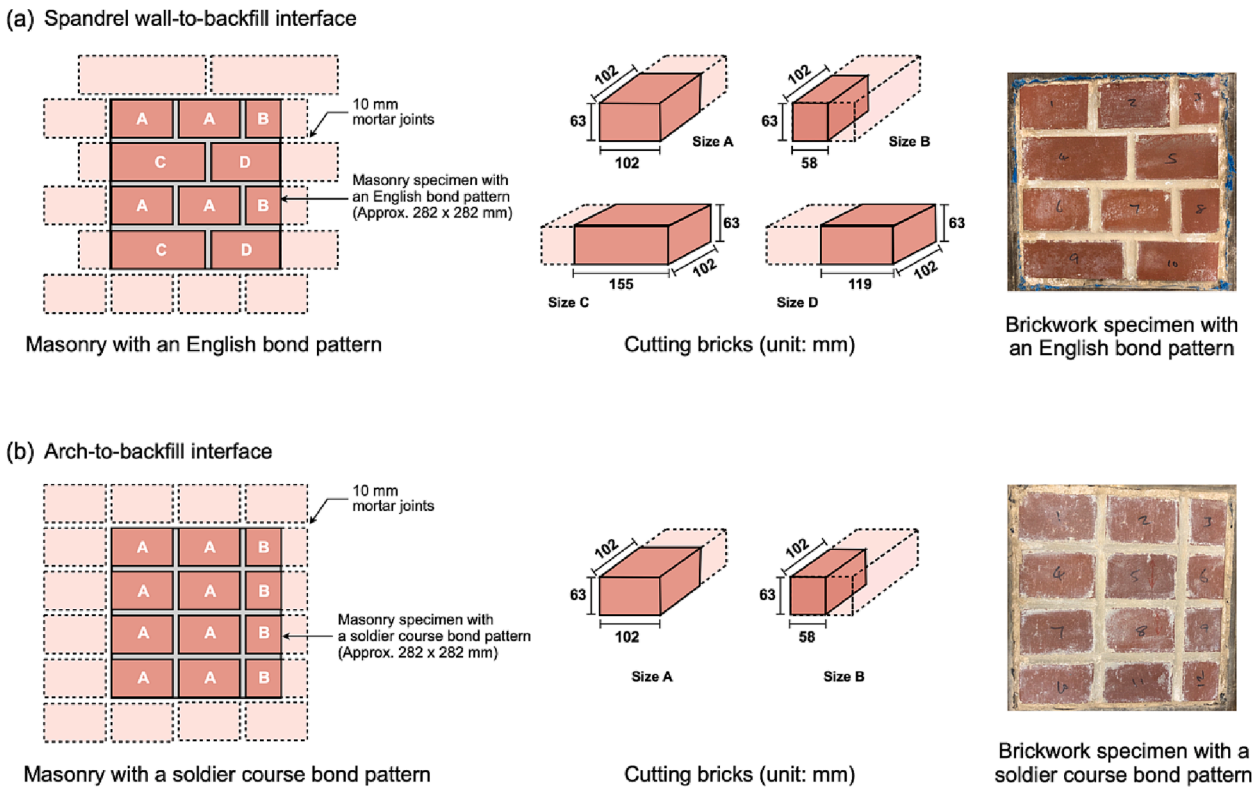

Fig. 2. Brickwork specimens (unit: mm). (a) Brickwork specimen with an English bond pattern to simulate the spandrel wall-backfill interface; (b) Brickwork specimen with a soldier course bond pattern to simulate the arch-backfill interface.

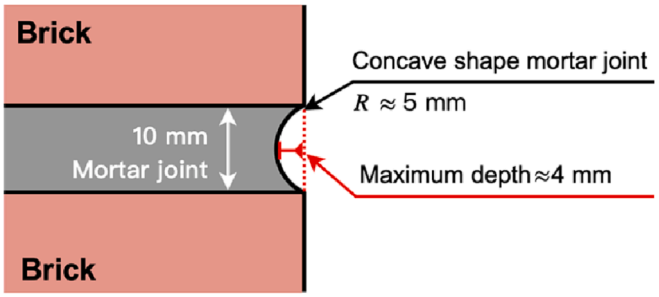

Fig. 3. Concave shape mortar joints.

Fig. 4. The puddling clay used in the study contained some mudstones and rock particles. Its index properties and grading curve are shown in Table 3 and Fig. 4, respectively [50–52].

To determine the shear properties (i.e., internal friction angle and cohesion) of the limestone and clay, a series of direct shear box tests were carried out. More specifically, a large shear box (Fig. 5 (a)) was used for the direct shear tests on limestone to meet the requirements outlined [53], such as that the length of the shear box should be at least ten times larger than the maximum particle diameter of the soil. The large shear box employed was 300 mm square with a thickness of 200 mm. A steel plate with grids at the inner surface was placed on top of the sample for the application of normal stress. Shear displacement was controlled by a belt-driven motor that pushes or pulls the lower shear box horizontally along slide tracks. Movement of the upper shear box was prevented by a horizontal arm fixed to the external box. During the pre-testing compression and shearing, a proving ring mounted between the arm and the lower shear box was used to measure the shear force applied, and two LVDTs were used for measuring the vertical deformation of the sample and the horizontal displacement of the lower shear box, respectively.

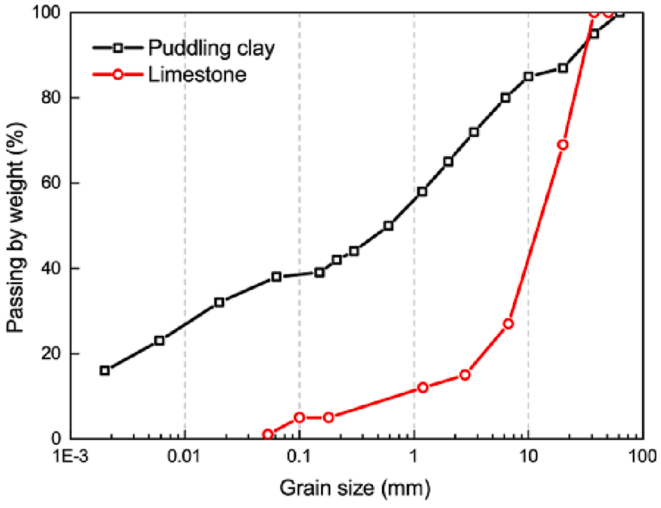

Fig. 4. Particle-size distribution of the limestone and puddling clay used in the study.

Table 3
Summary of main characteristics of the puddling clay used.

Property	Value/classification
Classification	Lean Clay (CL)
Natural moisture content	11%
Liquid limit	32%
Plastic limit	17%
Plasticity index	15%
Maximum dry density	1,840 kg/m^3

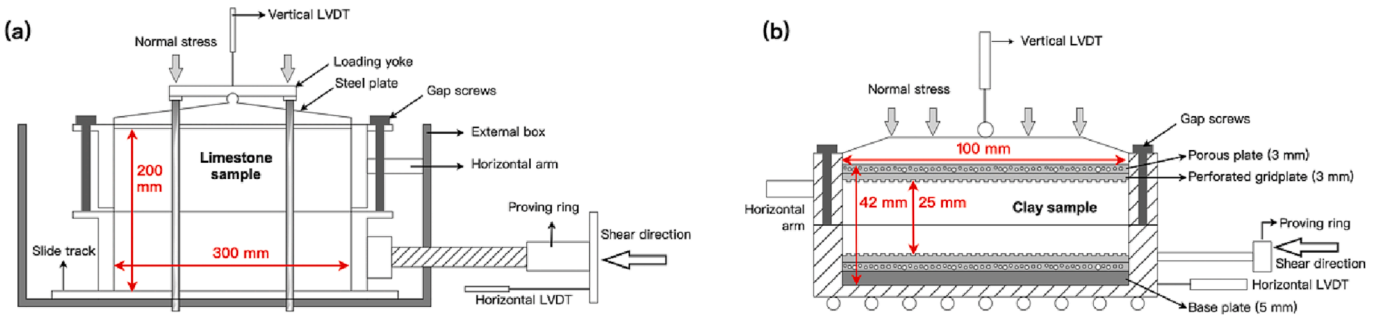

Fig. 5. (a) Large shear box apparatus for testing limestone; and (b) small shear box apparatus for testing clay.

Six direct shear box tests on limestone were performed under three levels of normal stress (115 kPa, 170 kPa, and 226 kPa), with two repetitions at each normal stress level to check the repeatability of the results. The same normal stress levels were adopted in the direct shear box tests on limestone as in the interface shear tests between brickwork specimens and backfill materials; the rationale for adopting these normal stress levels will be discussed in section 3.1. Given that the maximum particle diameter of limestone is approximately 25 mm, the thickness of the limestone sample was set to be 200 mm, the full capacity of the large shear box, to meet the requirement that the minimum specimen thickness shall be no less than six times the maximum grain diameter [54]. For the sampling and testing procedure, a total of 28 kg of limestone was placed into the shear box in four separate layers for each test. Each sample was manually compacted evenly by striking a 300 mm long, 50 mm width timber plate with a hammer to approximately reproduce the dense state of the backfill found in real masonry arch bridges. After all limestone was placed into the shear box, the target normal stress was applied via a steel plate placed on top of the sample for pre-compression. No significant volume change in the limestone observed after approximately 5 mins of compression due to its incompressible behaviour. The bulk density of limestone after compression was determined to be equal to 1,919 kg/m^3 with a CV equal to 2.0%. Before shearing, the upper shear box was raised around 5 mm against the lower box by turning four gap screws fitted in the four corners of the upper box. During shearing, the lower shear box was moved horizontally at a rate of 1 mm/min until a total displacement of at least 20 mm was achieved. It is worth noting that the constant normal stress was kept applied to the sample during the whole process of pre-compression, uplifting of the upper box, and shearing.

Considering that: a) the size of the shear box does not affect the accuracy of the characterisation of soil shear properties as long as the requirements outlined in [54] are satisfised; and b) with a smaller size shear box and lower volume of clay, the quality of compaction can be more easily controlled, a small shear box was used for testing the clay under consolidated drained conditions (see Fig. 5 (b)). It is worth noting that the clay sample during testing was in its natural state, which means that it had a natural moisture content and was not fully saturated (i.e., the clay is unlikely to be fully saturated unless the bridge has been flooded for a long period). This was to ensure the experimental results were representative of the behaviour of the clay in the field. Nevertheless, any large particles of mudstone or rock were removed from the clay sample before testing to minimize inconsistencies due the size of the shear box used.

A total of six tests were performed on clay samples at three levels of normal stresses (50 kPa, 111 kPa, and 167 kPa) with two repetitions under each normal stress to ensure consistency. The sample preparation and testing procedure were as follows: firstly, approximately 380 g of clay was weighed from a sealed plastic bag. The sample was then placed into a clean shear box over a set of porous and perforated grid plates. After that, the sample was manually compacted until its thickness reached approximately 25 mm. Another set of porous and perforated grid plates were placed on top of the sample following the manual compaction. Then, the shear box was installed in the apparatus, with the loading yoke hooking onto the lower shear box. Immediately after assembly of the shear box, the target constant normal load was applied for 3 days (the clay consolidation time was set to be the same as that for brickwork-clay interface shear tests), and the vertical deformation was monitored. After three days of consolidation, the volume change of the sample was recorded, and the average density of clay was determined to be 1,716 kg/m^3 with a CV equal to 6.7%. Before shearing, the upper and lower boxes were unlocked by removing two clamping screws and separated slightly by turning two gap screws. Finally, the sample was sheared at a low rate of 0.300 mm/min. The maximum horizontal displacement was 15 mm. LVDTs were used to measure the vertical deformation and horizontal displacement. The shear force was recorded by a load cell with a capacity of 2 kN placed between the lower shear box and the horizontal arm. The moisture content of the clay was measured after each test. Over the 26-day test, the moisture content of clay decreased slightly, ranging from 10.44% to 9.09%.

3. Brickwork-backfill interface shear strength tests

To accommodate the brickwork specimens, the large-scale shear box was used for the brickwork-backfill interface shear strength tests, and the configuration of the modified apparatus is shown in Fig. 6. The shear response of the brickwork-backfill interfaces, including the soldier course brickwork-limestone (SL) interface, soldier course brickwork-clay (SC) interface, English bond brickwork-limestone (EL) interface, and English bond brickwork-clay (EC) interface, were investigated. For each brickwork-backfill combination, three levels of normal stress were applied, and two repetitions of each test were carried out to check the repeatability of the results. In total, 24 interface shear tests were performed.

3.1. Determination of normal stress levels

The levels of normal stress applied in interface shear box tests were determined to represent real stress conditions found on masonry arch bridges. Assuming zero pore water pressures (neglecting any soil suc-

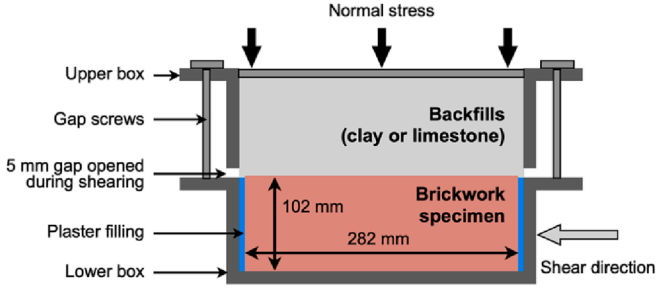

Fig. 6. Large shear box for brickwork-backfill interface shear tests.

tion), effective stresses are assumed to be equal to total stresses. Given the depth of backfill at the arch vault is H, the vertical total stress, S_v, at the arch barrel can be calculated as:

$$S_v = \gamma \bullet H \tag{1}$$

where γ is the unit weight of the backfill material.

A smooth interface between spandrel wall-backfill has been assumed to obtain approximate estimates of operational stresses. Now, based on the Rankine's theory [55], the passive lateral soil pressure P_p acting on the spandrel wall at the depth of H can be expressed as:

$$P_p = \gamma H K_p + 2c\sqrt{K_p} \tag{2}$$

where K_p, the passive lateral earth pressure coefficient, is related to the internal friction angle of soil (φ) and can be obtained by:

$$K_p = \tan^2\left(45 - \frac{\varphi}{2}\right) \tag{3}$$

Assuming that a masonry arch bridge has a backfill depth over the crown of the arch barrel equal to 1 m [56], and assigning typical values of 20 kN/m^3 and 40 $^\circ$ for γ and φ of the backfill (cohesionless) respectively, the passive vertical soil pressure on the arch barrel was calculated to be equal to 20 kPa, as per Eq.1. The full passive condition could give 92 kPa lateral pressure on spandrel walls (Eq.2). If an active action of passing vehicles was taken into consideration, additional active pressures would be applied to the arch barrel vertically and spandrel wall horizontally, depending on the weight and speed of the vehicle, and could reach a peak of 500 kPa at the spandrel wall and diminishes with distance from the load (for an analytical solution of the lateral stress acting on a retaining wall caused by a horizontal line load on a backfill see [57]). Considering the real stress state of a masonry arch bridge analysed above and the capacity of the large-scale shear box, the three levels of normal stresses for the interface shear tests were determined to be 115 kPa, 170 kPa, and 226 kPa, respectively.

3.2. Interface shear test procedures

After 30 days of curing, the brickwork specimen was placed in the lower half of the large shear box. The dimensions of the brickwork specimens were approximately 282 mm long × 282 mm wide × 102 mm high, allowing them to be perfectly accommodated by the lower shear box. There was a gap of approximately 9 mm between the specimen and the walls of the shear box, which was filled with plaster so that the specimen was fixed in position after the plaster had become solid (Fig. 6). Following installation of the brickwork specimen, a certain amount of backfill material (15.9 kg of limestone or 16.6 kg of puddling clay) was placed in the upper shear box in three separate layers. Each placement was followed by manual compaction to achieve a dense state of backfill, in line with the soil conditions found in real masonry arch bridges. It should be noted that the same masonry specimen was used for the 12 interface shear tests (6 tests with limestone and 6 tests with clay) to maintain similar surface roughness and texture. Then, the tested masonry specimen was removed, and another specimen with a different bond type was installed.

After placing the backfill material into the upper box, the testing procedures were different for the limestone and clay cases. For the brickwork-limestone interface tests, the procedures for pre-compression and shear were the same as those for the direct shear box tests on limestone. On the other hand, the brickwork-clay interface tests were performed under consolidated drained conditions. The states of the clay samples in the interface shear tests were the same as those in the direct shear box tests on clay, both being the natural states of the puddling clay.

Fig. 7 shows a typical consolidation curve for clay under constant normal stress. Clay was compressed sharply as a normal load was applied due to the air extrusion and the grid plate bedding into the sample. The second phase represents the clay consolidation with the dissipation of excess pore pressure. Clay was assumed to be fully consolidated when no significant volume change was observed. The time to 100% consolidation largely depends on the availability of drainage paths around the sample. In this study, the clay was surrounded by the masonry underneath and steel plates around and above. Limited drainage paths could result in the clay taking considerable time to reach 100% consolidation. To determine the clay consolidation time, the first test was started after 7-days of consolidation under the normal stress of 115 kPa. Then, the test was repeated in the same loading conditions but with the consolidation time reduced from 7-days to 3-days. Since no significant difference was observed in peak interface shear stress and shear stress versus horizontal displacement, the consolidation time for brickwork-clay interface shear tests was set to be 3 days for the rest of the tests considering the feasibility of the tests under laboratory conditions. A low shear rate of 0.300 mm/min was adopted to minimize the influence of excess pore pressure during shearing. The minimum horizontal displacement was 20 mm, which was 6.7% of the sample size.

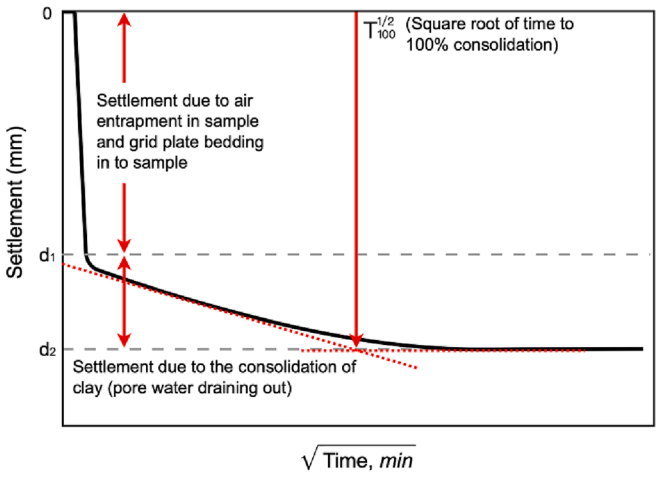

Fig. 7. Clay consolidation curve under a constant normal stress.

The average density of the consolidated clay was determined to be equal to 2,035 kg/m^3 with a CV of 1.8%. Also, the moisture content of the clay samples tested in the large shear box decreased from 11.90% (day 0) to 10.31% (day 96), see Fig. 8. Values of clay density and moisture content obtained from twelve interface shear tests between brickwork specimens and the clay backfill were similar, suggesting that

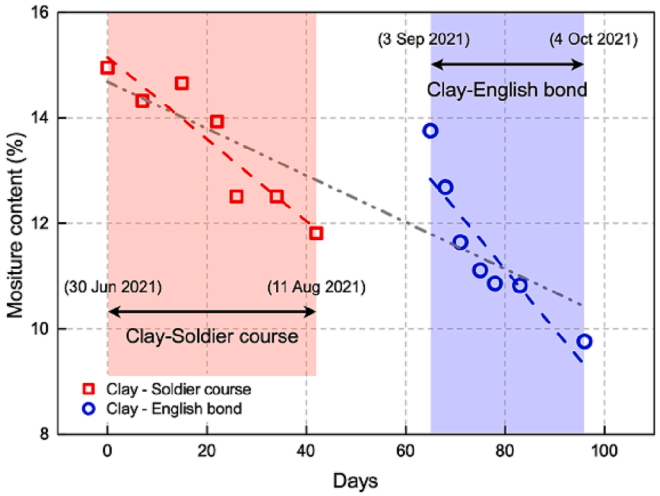

Fig. 8. Moisture content of clay during the shear tests on masonry-clay interfaces.

similar clay conditions were achieved.

4. Experimental results

4.1. Direct shear test results on clay and limestone

A total of twelve direct shear tests were carried out on two backfill materials under three different levels of normal stress, with two repetitions under the same conditions. Results from the small-scale direct shear tests on clay are shown in Fig. 9. Fig. 9(a) shows the shear strength and linear regression analysis results, together with the coefficient of determination (R^2). φ of clay was determined to be 37.2 ° and c was 30 kPa. The friction angle of the clay obtained is higher than expected for normal clay, which was attributed to the fact that the natural clay sample used in this study contained some larger particles. The failure of the clay was a ductile type under the normal stress of 111 kPa, whereas a peak stress followed by the strain-softening behaviour was observed under the normal stress of 50 kPa and 167 kPa, as shown in Fig. 9(b). Fig. 9(c) shows the vertical displacement versus the horizontal displacement during shearing. At low normal stress, the clay sustained a slight volume contraction under shear, followed by a dilation phase, while under the normal stress of 111 kPa, the contraction of the sliding surface was more pronounced. From Fig. 9(c), it can be seen that the volumetric response of clay under a normal stress of 167 kPa was less repeatable compared to that under the other two levels of normal stress. For one test, the sample tended to dilate from the beginning, whereas the other sample initially contracted and then slightly dilated. This type of variability in volumetric response has also been reported in previous studies [19]. The volumetric response of the soil under shear is closely related to the particle movements at the shear zone [58]. The difference in dilative/contractive behaviour may be attributed to the difference in shear zone thickness in different tests. Also, the greater randomness of the granular properties of the natural clay adopted in the study compared to the reconstituted clay could also make this difference more pronounced.

Fig. 10 shows the large-scale direct shear test results on limestone. In Fig. 10(a) the shear strength envelope suggests that the φ value of limestone was equal to 47.8 ° with the zero-cohesion assumption. Fig. 10(b) demonstrates that the shear failure of limestone was ductile, with no obvious peak point observed. The shear stress gradually increased during shearing and reached a critical state at a shear strain of approximately 6% to 10%. Both the vertical displacement and the peak shear stress of limestone showed very good agreement between the two tests under the same normal stress. Moreover, Fig. 10(c) suggests that the limestone tended to contract slightly at the beginning and then underwent considerable dilation until the end of the tests. The maximum vertical dilation was measured to be 8 mm. This significant volume dilation can be explained by the particle movement mechanism of limestone during shearing. The manual compaction and pre-compression make the limestone denser, with a great degree of interlock between particles. At the same time, the limestone contained several large particles with an angular shape, leading to great particle–particle friction. These factors result in the limestone grains at the slip plane being not only able to slide during shearing but also to tumble and lift. The rearrangement of particles at the slip plane requires much energy and could result in an increase in the volume of limestone during shearing [59].

4.2. Experimental results on brickwork-backfill interfaces

A total of twenty-four interface shear tests were carried out on four types of brickwork-backfill interfaces under three different levels of normal stress, with two repetitions under the same conditions. After the tests, no damage was observed in the brickwork specimens, indicating that the surface roughness and texture of brickwork specimens remained consistent over multiple tests. Previous studies have demonstrated that soil density can significantly impact the interface shear behaviour [60,61]. Table 4 summarises the values of soil density achieved after pre-test compaction for the limestone and after 3-days of consolidation for the clay. It can be seen that the variation of density is very small, with a maximum CV of less than 2%, indicating that similar soil conditions were achieved, and the effect of backfill density variation on the interface behaviour between brickwork and backfill can be assumed to be negligible.

Experimental results obtained from the four types of brickwork-backfill interfaces are summarized in Table 5, including mean values and corresponding CVs of shear strength under three levels of normal stress. Overall, very similar shear strengths were obtained from two repetitions of the test under the same conditions, indicating a high degree of repeatability of the experimental results.

Results from the interface shear tests between clay and brickwork constructed with an English bond pattern are illustrated in Fig. 11. From the shear strength envelope and the linear regression analysis (Fig. 11(a)), the EC interface had a friction angle of 14.5 ° with a cohesion intercept of 16.7 kPa. Under the zero-cohesion assumption, φ_i increased to 19.2 °. The shear stress increased with the horizontal displacement increase and reached a peak after 4 mm to 5 mm displacement (1.3% to 1.7% shear strain), followed by a slight decrease in residual shear strength for the further displacement (See Fig. 11(b)). The vertical displacement versus horizontal displacement curves (Fig. 11(c)) are less

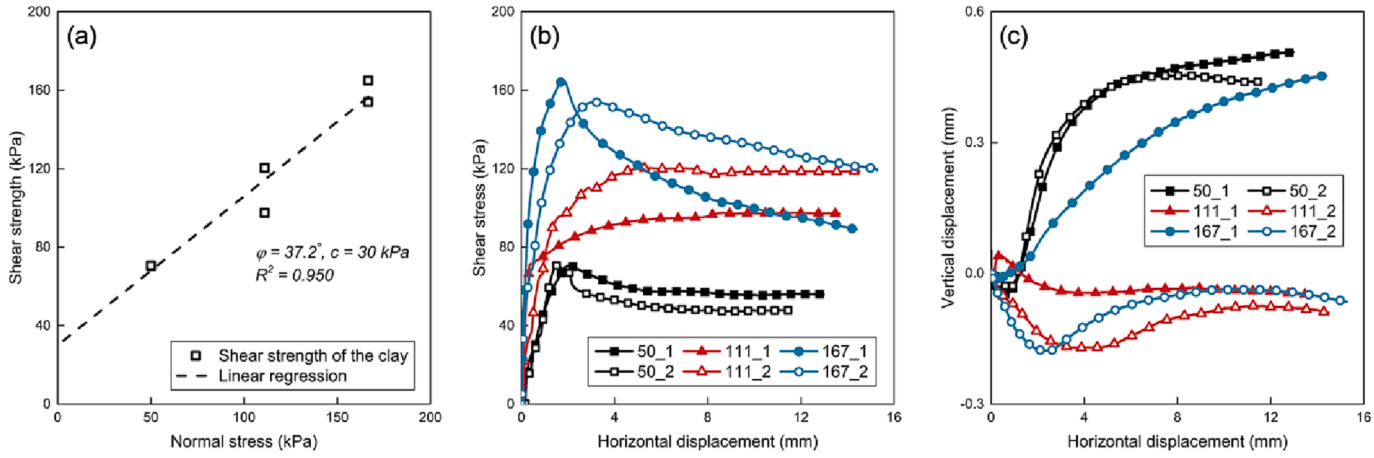

Fig. 9. Experimental results of small-scale direct shear tests on clay. (a) Shear strength envelope; (b) shear stress versus horizontal displacement; and (c) vertical displacement versus horizontal displacement.

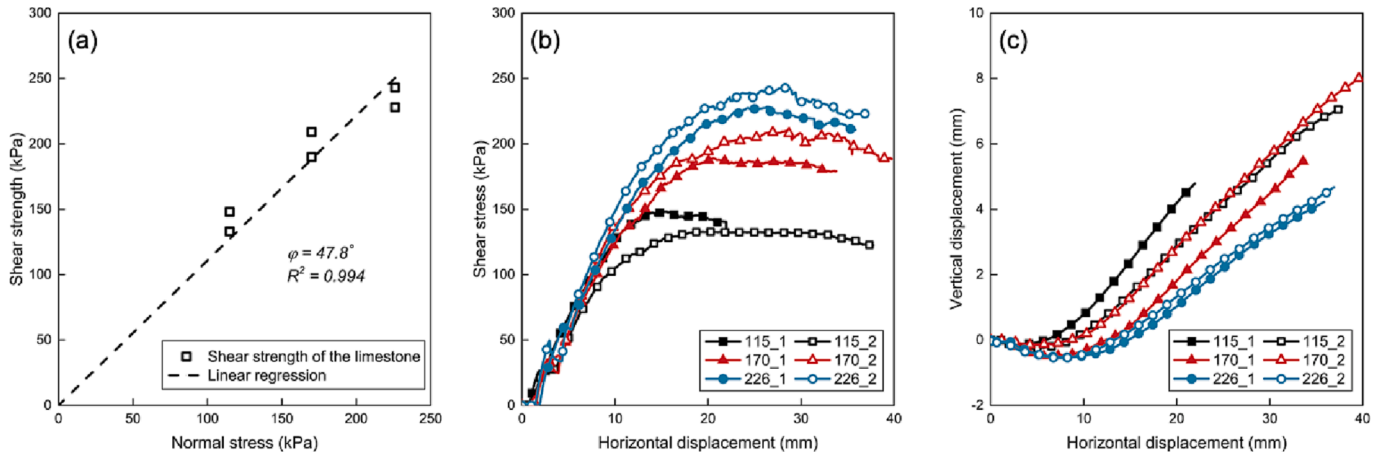

Fig. 10. Experimental results of the large-scale shear box tests on limestone. (a) Shear strength envelope; (b) shear stress versus horizontal displacement; and (c) vertical displacement versus horizontal displacement.

Table 4
Density of the backfill materials after consolidation (before shearing).

Interface	Brickwork bond pattern	Type of backfill	Number of tests	Density of the backfill after consolidation, before shearing	
				Mean value (kg/m^3)	CV
EC	English bond	Clay	6	2,021	1.4%
SC	Soldier course	Clay	6	2,048	2%
EL	English bond	Limestone	6	1,865	1.2%
SL	Soldier course	Limestone	6	1,876	Less than 1%

repeatable than the peak shear stress and shear stress development. The upper half of clay samples underwent a slight contraction within 0.2 mm during shearing, except for the one test under 226 kPa normal stress where the contraction of the clay sample reached up to 0.68 mm.

Experimental results on the SC interface are shown in Fig. 12. Fig. 12 (a) illustrates φ_i of 12.9 ° and c_i of 20.9 kPa at the SC interface. The assumption of zero-cohesion at the interface could result in an increase in φ_i to 18.9 °. Shear stress curves (Fig. 12(b)) showed a peak behaviour that the interface shear stress increased and reached a peak after a horizontal displacement of 2 to 3 mm (less than 1% of the shear strain). After the peak, a reduction in residual shear strength was observed, indicating strain-softening behaviour at the sliding plane. Moreover, the vertical deformation of clay samples exhibited a certain degree of variability across the tests (Fig. 12(c)). The clay dilated under lower normal stresses, and the dilation of the samples decreased as the normal stress increased. However, for the two tests at 170 kPa and 226 kPa normal stress, respectively, the clay samples contracted from the beginning of shearing.

Shear testing results on the EL and SL interfaces are shown in Figs. 13 and 14, respectively. The value of φ_i at the EL interface was determined to be 33.3 ° with a zero-cohesion assumption from the shear strength envelope shown in Fig. 13(a). For the SL interface, φ_i increased slightly to 35.7 ° (Fig. 14(a)). The shear strength and shear stress development show a very good agreement for the two tests under the same conditions. The EL and SL interfaces have a similar ductile failure type. Specifically, interface shear stress increased with the increment in the horizontal displacement and reached a peak after shearing approximately 9 to 11 mm (3.0% to 3.7% of the sample size). No noticeable reduction in residual shear strength was observed, indicating the post-peak strain-softening behaviour was marginal (See Fig. 13 (b) and 14 (b)). Regarding the volumetric response of the limestone, Fig. 13(c) and 14 (c) suggested that the limestone underwent a slight contraction and then dilation after the shear failure occurred.

5. Discussion

5.1. Influence of bond patterns on the shear behaviour of brickwork-backfill interface

For a continuous surface, it has been identified that surface roughness can significantly affect the interface resistance between soil and construction materials [9,64]. For example, by shearing Kawasaki clay against steel with different roughness, Tsubakihara et al. [62] found that, for smoother surfaces, the interface sliding occurred at the peak stress, followed by a reduction in residual strength. Conversely, when the surface roughness of steel was increased, shear failure occurred within the sand rather than at sand-steel interfaces, which means that the residual strength stays as the peak value. Subsequently, Hu and Pu [63] observed that the critical roughness of a surface is not only related to R_{max}, the absolute vertical distance between the highest peak and lowest valley along the surface profile, but can also be affected by the particle size of the soil. Therefore, a relative critical roughness, R_{cr}, can

Table 5
Summary of the interface shear test results.

Interface	Brickwork bond pattern	Type of backfill	Mean value and (CV) of the shear strength (kPa)			φ_i(°)	c_i(kPa)
			σ_n = 115 kPa	σ_n = 170 kPa	σ_n = 226 kPa		
EC	English bond	Clay	47.2 (3.0%)	58.9 (4.2%)	76.0 (7.5%)	14.5	16.7
						19.2	0
SC	Soldier course	Clay	48.2 (1.4%)	57.6 (2.5%)	73.6 (3.3%)	12.9	20.9
						18.9	0
EL	English bond	Limestone	87.4 (2.6%)	106.2 (9.7%)	146.2 (4.0%)	33.3	0
SL	Soldier course	Limestone	84.6 (7.0%)	120.5 (3.4%)	162.8 (1.0%)	35.7	0

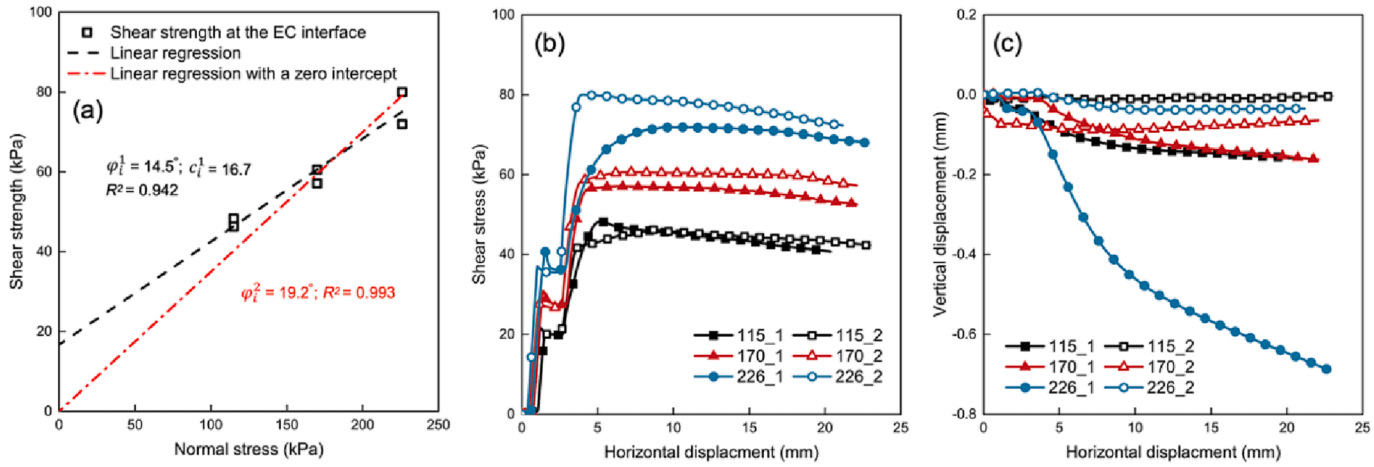

Fig. 11. Experimental results on EC interface. (a) Shear strength envelope; (c) shear stress versus horizontal displacement; and (d) vertical displacement versus horizontal displacement.

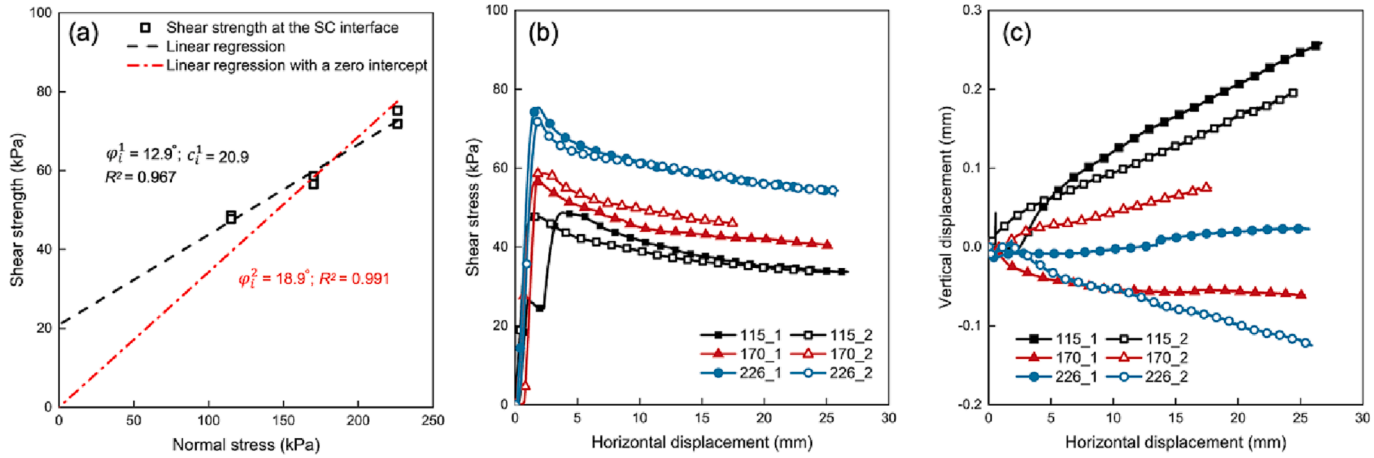

Fig. 12. Experimental results on SC interface. (a) Shear strength envelope; (b) shear stress versus horizontal displacement; and (c) vertical displacement versus horizontal displacement.

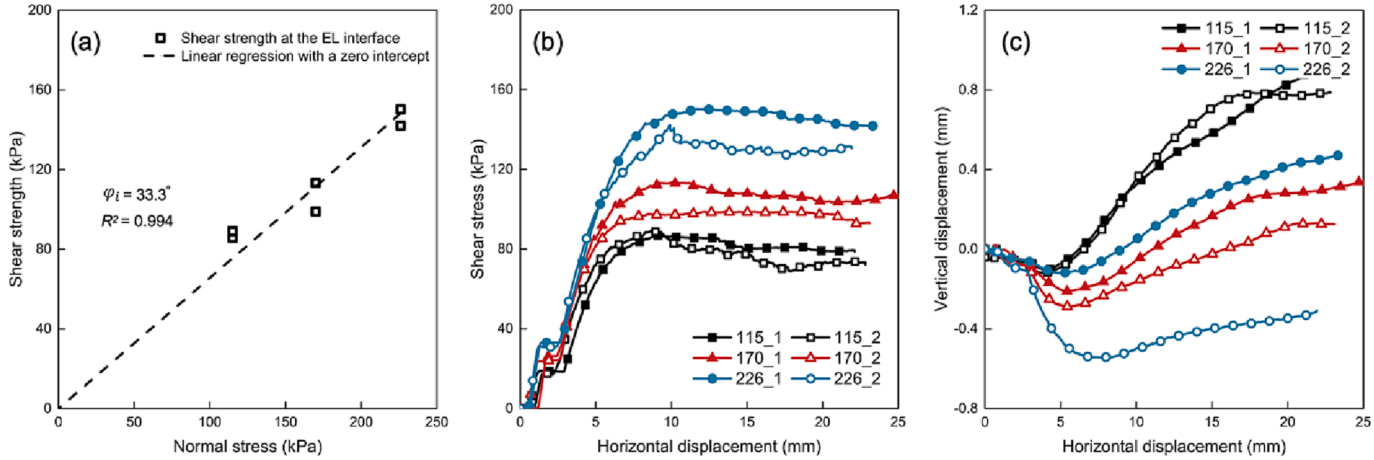

Fig. 13. Experimental results on EL interface. (a)Shear strength envelope; (b) shear stress versus horizontal displacement; and (c) vertical displacement versus horizontal displacement.

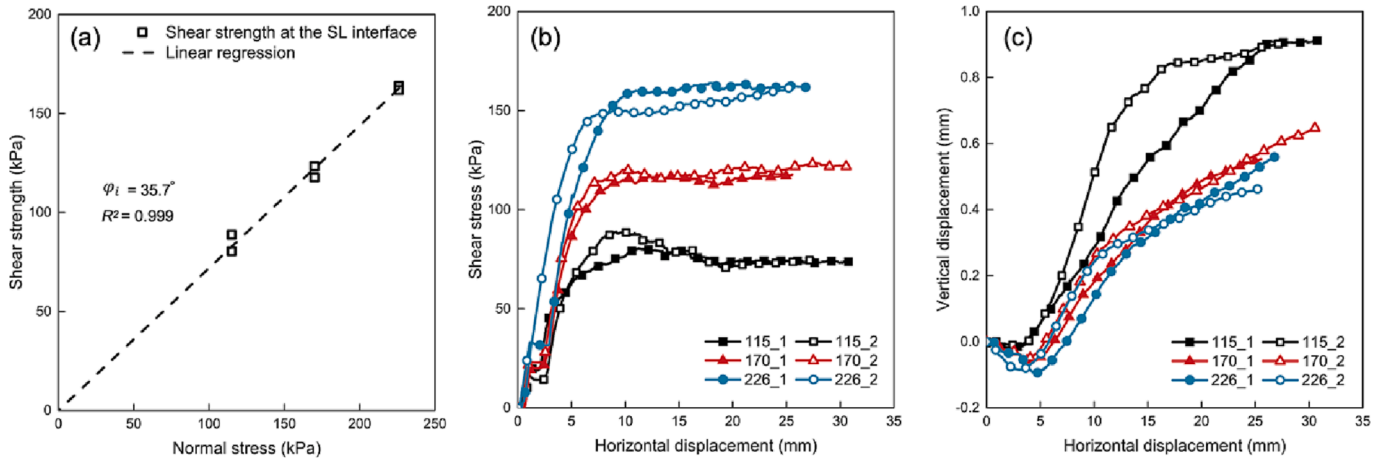

Fig. 14. Experimental results on SL interface. (a) Shear strength envelope; (b) shear stress versus horizontal displacement; and (c) vertical displacement versus horizontal displacement.

be used to describe how the surface roughness and particle size affect the shear behaviour of the soil-structure interface. R_{cr} can be expressed by the following equation:

$$R_{cr} = R_{max}/D_{50} \tag{4}$$

where D_{50} represents the average particle size of a soil.

For brickwork, the surface roughness of bricks, the profile of mortar joints, and the joint arrangement can affect its surface roughness and texture. The former two factors could be deemed identical for the two masonry specimens used in this study due to the usage of the same materials and construction methods. However, the different layouts of joints in the two masonry specimens result in different textures, which may further affect their shear behaviour at the brickwork-backfill interface. Based on the experimental results obtained from EL, SL, EC, and SC interfaces, there were no statistically significant differences found to indicate that the joint layout of the brickwork had a significant effect on the frictional properties of the four interfaces investigated in this study.

For the brickwork and clay combinations (EC and SC interfaces), their shear stress-displacement relationships (Fig. 11 (b) and Fig. 12 (b)) suggest that the shear behaviour of the brickwork-clay interface was in line with the typical shear behaviour of soil against a relatively smooth surface (i.e., the shear stress had a peak behaviour, the residual strength decreased, and shear failure occurred at the brickwork-clay contact interface) [62]. On the other hand, Fig. 11(a) and Fig. 12(a) demonstrate that the shear strength obtained at the EC interface was approximately 2.2% and 3.2% greater than that at the SC interface under normal stresses of 170 kPa and 226 kPa, respectively. Also, φ_i at the EC interface

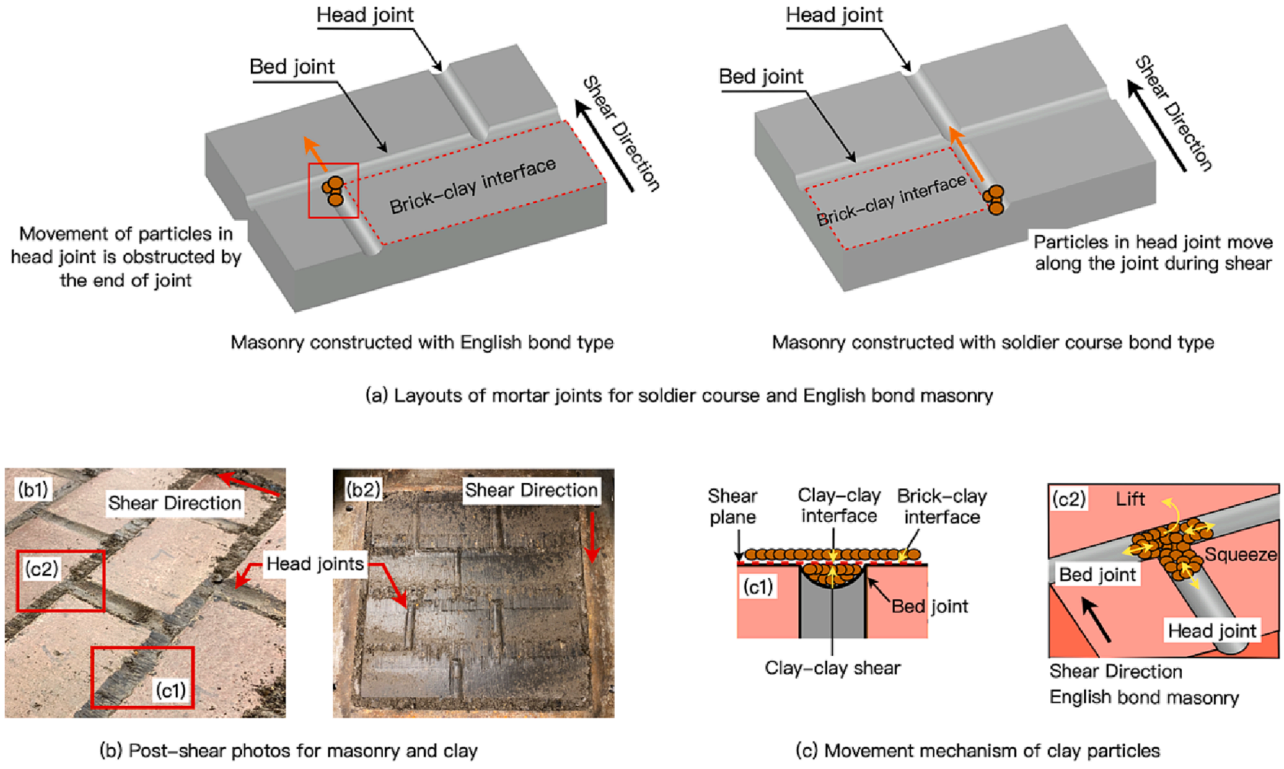

Fig. 15. (a) Layouts of mortar joints for the soldier course and English bond masonry; (b) post-shear photos for brickwork with an English bond pattern and clay; and (c) movement mechanism of clay particles during shear.

was always greater than that at the SC interface, irrespective of whether zero-cohesion at the interface was assumed. For instance, φ_i at the EC interface was 12.4% and 1.6% greater than that at the SC interface when cohesion or zero cohesion was considered, respectively.

The larger shear strength and φ_i obtained from the EC interface compared to those obtained from the SC interface may, to some extent, reflect how the joint layout affects the shear behaviour of the brickwork-clay interface by influencing particle movement at the sliding plane. Specifically, clay particles fill in the concave joints under normal compression. During shearing, the clay over the bricks shears against the surface of the brick, forming the clay-brick interface. For clay particles filling the bed joints (perpendicular to the shear direction), the shear causes their movement to be obstructed by the bed joints, so that the shear failure occurs within the clay, creating clay-clay interfaces (see Fig. 15(c1)), which can be evidenced by the post-shear image of the masonry specimen shown in Fig. 15(b). Regarding the effect of head joints (parallel to the shear direction) on the clay movement, the head joints of the brickwork constructed with the soldier bond type are aligned, allowing clay particles embedded into the head joints to move along the joint under shearing (Fig. 15(a)). However, for the brickwork constructed with the English bond pattern, head joints are interrupted by several equally spaced bed joints. Thus, the movement of clay particles may be restricted, which could trigger lifting and squeezing of the particles during their rearrangement (see Fig. 15(c2)). The more complex movement and rearrangement of clay particles at the EC interface would then require more energy, resulting in the EC interface having a larger shear strength and interface friction angle compared to those of the SC interface [64].

However, for the brickwork and limestone combinations (EL and SL interfaces), the experimental results were inconsistent with the results obtained from brickwork-clay interfaces. Specifically, the values of shear strength obtained from the EL interface were smaller than those from SL interface under normal stresses of 170 kPa and 226 kPa, and the value of φ_i for the EL interface was also slightly smaller than that for the SL interface (see Fig. 13 (a) and Fig. 14 (a)). The main reason for the inconsistency between the results from brickwork-clay interfaces and brickwork-limestone interfaces was the fact that the particle size of limestone was significantly larger than that of the clay used (Fig. 2). The larger limestone particle sizes resulted in the R_{cr} between brickwork and limestone to become smaller than that between brickwork and clay. As a result, shear failure occurred within the limestone rather than at the brickwork-limestone interface. This was confirmed by the shear stress development curves obtained from the EL and SL interfaces (see Fig. 13 (b) and 14 (b)), which showed a ductile failure, without any significant decrease in residual shear strength [62].

5.2. Influence of backfill properties on the shear behaviour between brickwork-backfill interfaces

The force transfer mechanisms for cohesive soils and non-cohesive soils are different. The force transfer mechanism in clay is primarily through the inter-particle bonding, which is due to the cohesive forces between clay particles. Conversely, the transfer of forces in limestone is primarily through friction between the particles [65]. These different force transfer mechanisms result in the shear behaviour between the brickwork-limestone interface and brickwork-clay interface to differ. The results of the current study are overall in agreement with previously published findings on interface shear tests between sand-clay mixtures and structural surfaces [24,66]. Specifically, brickwork-clay interfaces had a lower φ_i than brickwork-limestone interfaces. For example, assuming zero-cohesion at masonry-backfill interfaces, φ_i between clay and brickwork was approximately 55% smaller than that between limestone and brickwork. From the interface shear stress perspective, the peak shear stress at a brickwork-limestone interface was significantly larger than that at a brickwork-clay interface due to the interlock behaviour involving limestone particles and the brickwork-limestone interface. Moreover, the tangential deformation at failure for the brickwork- limestone interface was also significantly larger than that for the brickwork-clay interface. For instance, it was observed that the critical tangential strains were 3.0% to 3.7% and 1.3% to 1.7% for the brickwork-limestone interface and brickwork-clay interface, respectively.

5.3. Comparison of the internal shear behaviour of backfills and interface shear behaviour between brickwork and backfill

Generally, as the surface roughness increases, shear failure at the soil-structure interface occurs from fully sliding along the contact interface (for very smooth interfaces) to the interior of the soil, which results in an interface shear behaviour close to the soil-soil shear behaviour [67]. The results of the present study indicate several differences in shear behaviour between the backfill and brickwork-backfill interfaces. Firstly, the shear strength of brickwork-backfill interfaces was significantly lower than that of the backfill materials under the same normal stress. For example, the average shear strength of limestone was 63.4%, 76.0%, and 52.4% higher than that of the brickwork-limestone interfaces at normal stress of 115 kPa, 170 kPa, and 226 kPa, respectively. Similar results were observed for the clay and brickwork-clay interfaces. As for the shear strain, the critical shear strain obtained from the direct shear tests on limestone (6% to 10%) was almost twice as high as that from the brickwork-limestone interface shear tests (3% to 3.7%).

Table 6 summarises the ratio between φ_i of brickwork-backfill interfaces and φ of backfills. These ratios can be used as a guide by researchers and engineers when selecting friction parameters between brickwork and backfill materials when modelling masonry arch bridges. It can be seen from Table 6 that the values of $\varphi_i$are significantly smaller than φ of the corresponding backfill materials. Different bond types of masonry could result in different interface friction angles, but the difference in φ_i/φ due to the variation of masonry bond patterns was not pronounced. Therefore, the effects of masonry bond types may be negligible when assigning frictional parameters to the brickwork-backfill interfaces. However, Table 6 suggests that φ_i/φ is closely related to the types of backfill and the cohesion characteristics at brickwork-backfill interfaces, which has not been adequately considered in previous masonry arch bridge modelling studies (see Table 1). For example, taking limestone as the backfill material resulted in φ_i/φ ranging from 0.70 to 0.75 (most previous numerical studies adopted φ_i/φ within or close to this range, as suggested in Table 1). But when the clay was adopted as the backfill material, φ_i/φ was determined to be 0.35 to 0.39, when the interface cohesion was taken into consideration. The zero-cohesion assumption at the brickwork-clay interface led to an increase in φ_i/φ to approximately 0.5.

Table 6
Summary of shear parameters for backfills and brickwork-backfill interfaces.

Samples/interfaces		Friction angle (°)	Cohesion (kPa)	R^2	φ_i/φ
Clay		37.2	30.0	0.950	–
Limestone		47.8	0	0.994	–
EC interface	With cohesion	14.5	16.7	0.942	0.39
	Zero-cohesion	19.2	0	0.993	0.52
SC interface	With cohesion	12.9	20.9	0.967	0.35
	Zero-cohesion	18.9	0	0.991	0.51
EL interface		33.3	0	0.994	0.70
SL interface		35.7	0	0.999	0.75

6. Conclusions

The present study presents an experimental procedure to assess the interface shear behaviour between brickwork masonry and backfill materials. Thirty-six experimental tests were performed to investigate the internal shear behaviour of backfill materials and the interface shear behaviour between brickwork and backfill materials in masonry arch bridges. The brickwork specimens were constructed using Type A bricks with cement mortar to achieve good durability and to keep the surface texture of the specimen effectively unchanged for all 12 experiments carried out on each brickwork specimen. The friction angle and cohesion intercept of limestone, puddling clay, and four types of brickwork-backfill interfaces were characterised. Moreover, the effects of masonry bond patterns and backfill properties on the shear behaviour at brickwork-backfill interfaces were assessed. From the analysis of the results, the following conclusions can be drawn:

- For the brickwork and clay combinations, shear failure occurred at the brickwork-clay interfaces. In these cases, the bond pattern of brickwork was found to affect the movement of clay particles. The values of $\varphi_i$and shear strength obtained from the SC interface were smaller than those obtained from the EC interface due to the aligned joint arrangement of the brickwork specimens with a soldier course bond pattern. However, for the limestone, which had much larger particle sizes, shear failure occurred within the limestone and was of a ductile type. Nevertheless, in the cases investigated in the study, the influence of brickwork bond patterns on the shear behaviour at brickwork-backfill interfaces was not significant and may be considered negligible when assessing masonry arch bridges.
- The properties of the backfill materials had a marked impact on brickwork-backfill interface shear behaviour. The critical shear strain, peak shear stress and interface friction angle of brickwork-limestone interfaces were significantly larger than those of brickwork-clay interfaces.
- The internal angle of friction of the backfill materials was higher than the interface angle of friction between brickwork and backfill. On the other hand, backfill type was found to significantly affect the shear behaviour at the brickwork-backfill interface. In the case of limestone backfill, φ_i/φ ranged from 0.70 to 0.75. In the case of clay backfill, φ_i/φ was determined to be 0.51 to 0.52 under the assumption of zero-cohesion at the masonry-clay interface, or 0.35 to 0.39 if interface cohesion was taken into account. These ratios provide experimentally-derived parameters that researchers and practicing engineers can refer to when modelling masonry arch bridges numerically.

However, the results presented herein relate to the specific brickwork and backfill employed and different material combinations may furnish different outcomes. The results are strongly influenced by the relative roughness of the brickwork surface and the backfill, as well as the arrangement and profile of the mortar joints.

The results obtained from this study may provide researchers and engineers with a firm basis of the procedure to be undertaken to obtain the interface parameters between masonry and backfill.

CRediT authorship contribution statement

Bowen Liu: Writing – review & editing, Data curation, Writing – original draft, Visualization, Conceptualization, Methodology. **Anastasios Drougkas:** Writing – review & editing, Conceptualization, Methodology. **Vasilis Sarhosis:** Supervision, Conceptualization, Methodology, Writing – review & editing. **Colin C. Smith:** Supervision, Writing – review & editing. **Matthew Gilbert:** Supervision, Writing – review & editing.

Declaration of Competing Interest

The authors declare that they have no known competing financial interests or personal relationships that could have appeared to influence the work reported in this paper.

Data availability

Data will be made available on request.

Acknowledgements

This work was funded by the EPSRC project 'Exploiting the resilience of masonry arch bridge infrastructure: a 3D multi-level modelling framework' (ref. EP/T001348/1). The financial contribution is very much appreciated. Mr Ian Day is also acknowledged for his support towards the construction of the masonry specimens used in the experiments.

References

[1] Sarhosis V, De Santis S, De Felice G. A review of experimental investigations and assessment methods for masonry arch bridges. Struct Infrastruct Eng 2016;12:1439–64. https://doi.org/10.1080/15732479.2015.1136655.
[2] Sarhosis V, Sheng Y. Identification of material parameters for low bond strength masonry. Eng Struct 2014;60:100–10. https://doi.org/10.1016/j.engstruct.2013.12.013.
[3] Lourenço PB, Rots JG, Blaauwendraad J. Continuum model for masonry: parameter estimation and validation. J Struct Eng 1998;124:642–52. https://doi.org/10.1061/(ASCE)0733-9445(1998)124:6(642).
[4] A.W. Hendry, Masonry properties for assessing arch bridges, 1990.
[5] Drougkas A, Roca P, Molins C. Material Characterization and Micro-Modeling of a Historic Brick Masonry Pillar, International Journal of. Archit Herit 2016;10:887–902. https://doi.org/10.1080/15583058.2016.1157711.
[6] Bareither CA, Benson CH, Edil TB. Comparison of shear strength of sand backfills measured in small-scale and large-scale direct shear tests. Can Geotech J 2008;45:1224–36. https://doi.org/10.1139/T08-058.
[7] Pulatsu B, Erdogmus E, Lourenço PB. Comparison of in-plane and out-of-plane failure modes of masonry arch bridges using discontinuum analysis. Eng Struct 2019;178:24–36. https://doi.org/10.1016/j.engstruct.2018.10.016.
[8] M. Gilbert, C.C. Smith, T.J. Pritchard, Masonry arch analysis using discontinuity layout optimisation, Proceedings of the Institution of Civil Engineers - Engineering and Computational Mechanics. 163 (2010) 155–166. https://doi.org/10.1680/eacm.2010.163.3.155.
[9] S. Grosman, A.B. Bilbao, L. Macorini, B.A. Izzuddin, Numerical modelling of three-dimensional masonry arch bridge structures, Proceedings of the Institution of Civil Engineers - Engineering and Computational Mechanics. 174 (2021) 96–113. https://doi.org/10.1680/jencm.20.00028.
[10] Chen X, Zhang J, Xiao Y, Li J. Effect of roughness on shear behavior of red clay-concrete interface in large-scale direct shear tests. Can Geotech J 2015;52:1122–35. https://doi.org/10.1139/cgj-2014-0399.
[11] Sarhosis V, Forgács T, Lemos JV. A discrete approach for modelling backfill material in masonry arch bridges. Comput Struct 2019;224:106108. https://doi.org/10.1016/j.compstruc.2019.106108.
[12] Forgács T, Sarhosis V, Ádány S. Shakedown and dynamic behaviour of masonry arch railway bridges. Eng Struct 2021;228. https://doi.org/10.1016/J.ENGSTRUCT.2020.111474.
[13] Scozzese F, Ragni L, Tubaldi E, Gara F. Modal properties variation and collapse assessment of masonry arch bridges under scour action. Eng Struct 2019;199. https://doi.org/10.1016/J.ENGSTRUCT.2019.109665.
[14] Oliveira DV, Lourenço PB, Lemos C. Geometric issues and ultimate load capacity of masonry arch bridges from the northwest Iberian Peninsula. Eng Struct 2010;32:3955–65. https://doi.org/10.1016/J.ENGSTRUCT.2010.09.006.
[15] Bayraktar A, Hökelekli E. Seismic performances of different spandrel wall strengthening techniques in masonry arch bridges. Int J Archit Herit 2021;15:1722–40. https://doi.org/10.1080/15583058.2020.1719234.
[16] Bayraktar A, Hökelekli E. Nonlinear soil deformability effects on the seismic damage mechanisms of brick and stone masonry arch bridges. Int J Damage Mech 2021;20:431–52. https://doi.org/10.1177/1056789520974423.
[17] Pantò B, Chisari C, Macorini L, Izzuddin BA. A hybrid macro-modelling strategy with multi-objective calibration for accurate simulation of multi-ring masonry arches and bridges. Comput Struct 2022;265. https://doi.org/10.1016/J.COMPSTRUC.2022.106769.
[18] Taha A, Fall M. Shear Behavior of Sensitive Marine Clay-Concrete Interfaces. J Geotech Geoenvironm Eng 2013;139:644–50. https://doi.org/10.1061/(asce)gt.1943-5606.0000795.
[19] Yavari N, Tang AM, Pereira JM, Hassen G. Effect of temperature on the shear strength of soils and the soil–structure interface. Can Geotech J 2016;53:1186–94. https://doi.org/10.1139/cgj-2015-0355.

[20] Silva IN, Indraratna B, Nguyen TT, Rujikiatkamjorn C. Shear behaviour of subgrade soil with reference to varying initial shear stress and plasticity index. Acta Geotech 2022. https://doi.org/10.1007/s11440-022-01477-w.
[21] Han F, Ganju E, Salgado R, Prezzi M. Effects of interface roughness, particle geometry, and gradation on the sand-steel interface friction angle. J Geotech Geoenvironm Eng-ASCE 2018;144:1–12. https://doi.org/10.1061/(ASCE)GT.1943.
[22] Ho TYK, Jardine RJ, Anh-Minh N. Large-displacement interface shear between steel and granular media. Geotechnique 2011;61:221–34. https://doi.org/10.1680/geot.8.P.086.
[23] Rouaiguia A. Residual shear strength of clay-structure interfaces. International Journal of Civil & Environmental Engineering IJCEE-IJENS 2010;10:5–14.
[24] Yin K, Fauchille A-L, Di Filippo E, Kotronis P, Sciarra G. A review of sand–clay mixture and soil–structure interface direct shear test. Geotechnics 2021;1:260–306. https://doi.org/10.3390/geotechnics1020014.
[25] Lemos LJ, Vaughan PR. Clay-interface shear resistance. Geotechnique 2000;50:55–64.
[26] Ravera E, Laloui L. Failure mechanism of fine-grained soil-structure interface for energy piles. Soils Found 2022;62:101152. https://doi.org/10.1016/j.sandf.2022.101152.
[27] Uesugi M, Kishida H, Tsubakihara Y. Behavior of sand particles in sand-steel friction. Soils Found 1988;28:107–18. https://doi.org/10.3208/SANDF1972.28.107.
[28] Littleton I. An experimental study of the adhesion between clay and steel. J Terramech 1976;13:141–52.
[29] British Standard, BS EN 772 Methods of test for masonry units, 2001.
[30] ASTM C 496-85, Standard test method for splitting tensile strength of cylindrical concrete specimens, 2004.
[31] Potyondy JG. Skin friction between various soils and construction materials. Géotechnique 1961;11:339–53. https://doi.org/10.1680/geot.1961.11.4.339.
[32] O'Rourke TD, Druschel SJ, Netravali AN. Shear strength characteristics of sand-polymer interfaces. J Geotech Eng 1990;116:451–69. https://doi.org/10.1061/(ASCE)0733-9410(1990)116:3(451).
[33] Lee S. Influence of surface topography on interface strength and counterface soil structure. PhD Thesis, Georgia Institute of Technology 1998.
[34] Frost JD, DeJong JT, Recalde M. Shear failure behavior of granular–continuum interfaces. Eng Fract Mech 2002;69:2029–48. https://doi.org/10.1016/S0013-7944(02)00075-9.
[35] Dove JE, Frost JD. Peak friction behavior of smooth geomembrane-particle interfaces, Journal of Geotechnical and Geoenvironmental. Engineering 1999;125:544–55. https://doi.org/10.1061/(ASCE)1090-0241(1999)125:7(544).
[36] Tovar-Valencia RD, Galvis-Castro A, Salgado R, Prezzi M. Effect of surface roughness on the shaft resistance of displacement model piles in sand. J Geotech Geoenviron Eng 2018;144. https://doi.org/10.1061/(ASCE)GT.1943-5606.0001828.
[37] Kestell Floyer J. English brick buildings of the fifteenth century. Archaeological Journal 1913;70:121–32. https://doi.org/10.1080/00665983.1913.10853220.
[38] Cecchi A, Milani G. A kinematic FE limit analysis model for thick English bond masonry walls. Int J Solids Struct 2008;45:1302–31. https://doi.org/10.1016/j.ijsolstr.2007.09.019.
[39] T. Taguchi, C. Cuadra, Influence of bond types on brick masonry strength, in: The 2015 World Congress on Advances in Structural Engineering and Mechanics (ASEM15), Incheon, Korea, 2015.
[40] Milani G, Lourenço PB. 3D non-linear behavior of masonry arch bridges. Comput Struct 2012;110–111:133–50. https://doi.org/10.1016/j.compstruc.2012.07.008.
[41] Abdou L, Saada RA, Meftah F, Mebarki A. Experimental investigations of the joint-mortar behaviour. Mech Res Commun 2006;33:370–84. https://doi.org/10.1016/j.mechrescom.2005.02.026.
[42] Gambarotta L, Lagomarsino S. Damage models for the seismic response of brick masonry shear walls. Part I: the mortar joint model and its applications, Earthq Eng Struct Dyn 1997;26:423–39.
[43] Dorji J, Zahra T, Thambiratnam D, Lee D. Strength assessment of old masonry arch bridges through moderate destructive testing methods. Constr Build Mater 2021;278:122391. https://doi.org/10.1016/j.conbuildmat.2021.122391.
[44] Tubaldi E, Macorini L, Izzuddin BA. Three-dimensional mesoscale modelling of multi-span masonry arch bridges subjected to scour. Eng Struct 2018;165:486–500. https://doi.org/10.1016/J.ENGSTRUCT.2018.03.031.
[45] Cox D, Halsall R. Brickwork arch bridge. Berkshire, UK: The brick development association; 1996.
[46] Callaway P, Gilbert M, Smith CC. Influence of backfill on the capacity of masonry arch bridges. Bridg Eng 2012;165:147–58. https://doi.org/10.1680/bren.11.00038.
[47] Callaway PA. Soil-structure interaction in masonry arch bridges. University of Sheffield 2007.
[48] Melbourne C, Gilbert M. The behaviour of multiring brickwork arch bridges. Struct Eng 1995;73:39–47.
[49] Augusthus-Nelson L, Swift G. Experimental investigation of the residual behaviour of damaged masonry arch structures. Structures 2020;27:2500–12. https://doi.org/10.1016/j.istruc.2020.08.008.
[50] ASTM D4318-10, Standard test methods for liquid limit, plastic limit, and plasticity index of soils, 2010.
[51] ASTM D698-12, Standard test methods for laboratory compaction characteristics of soil Using standard effort, 2012.
[52] ASTM D2487-11, Standard practice for classification of soils for engineering purposes (unified soil classification system), West Conshohocken, PA, 2017. https://doi.org/10.1520/D2487-11.
[53] ASTM-2011, Standard test method for direct shear test of soils under consolidated drained conditions, 2011.
[54] AASHTO, T 236-08. Standard method of test for direct shear test of soils under consolidated drained conditions, American Association of State Highway and Transportation Officials. 3 (2018).
[55] Rankine W. On the stability of loose earth. Philos Trans R Soc Lond 1857;147:9–27. https://doi.org/10.1098/rstl.1857.0003.
[56] B. Pulatsu, E. Erdogmus, P.B. Lourenço, Influence of soil-backfill depth on the strength and behavior of masonry arch bridges in the transverse direction, in: 13th North American Masonry Conference, Salt Lake, UT, USA, 2019: pp. 16–19.
[57] Wang C-D. Lateral stress caused by horizontal and vertical surcharge strip loads on a cross-anisotropic backfill. Int J Numer Anal Methods Geomech 2005;29:1341–61. https://doi.org/10.1002/nag.462.
[58] Mandl G, De Jong LNJ, Maltha A. Shear zones in granular material. Rock Mech 1977;9:95–144.
[59] Rowe PW. The stress-dilatancy relation for static equilibrium of an assembly of particles in contact. Proc R Soc Lond A Math Phys Sci 1962;269:500–27.
[60] Abu-Farsakh M, Coronel J, Tao M. Effect of soil moisture content and dry density on cohesive soil–geosynthetic interactions using large direct shear tests. J Mater Civ Eng 2007;19:540–9. https://doi.org/10.1061/(ASCE)0899-1561(2007)19:7(540).
[61] Ferreira FB, Vieira CS, Lopes ML. Direct shear behaviour of residual soil–geosynthetic interfaces – influence of soil moisture content, soil density and geosynthetic type. Geosynth Int 2015;22:257–72. https://doi.org/10.1680/gein.15.00011.
[62] Tsubakihara Y, Kishida H. Frictional behaviour between normally consolidated clay and steel by two direct shear type apparatuses. Soils Found 1993;33:1–13. https://doi.org/10.3208/sandf1972.33.2_1.
[63] Hu L, Pu J. Testing and modeling of soil-structure interface. J Geotech Geoenvironm Eng 2004;130:851–60. https://doi.org/10.1061/(ASCE)1090-0241(2004)130:8(851).
[64] Han F, Ganju E, Salgado R, Prezzi M. Effects of Interface Roughness, Particle Geometry, and Gradation on the Sand-Steel Interface Friction Angle. J Geotech Geoenviron Eng 2018;144. https://doi.org/10.1061/(ASCE)GT.1943.
[65] Kim UG, Hyodo M, Koga C, Orense RP. Effect of fines content on the monotonic shear behavior of sand-clay mixtures. Ube, Japan: CRC Press; 2006.
[66] Dafalla MA. Effects of clay and moisture content on direct shear tests for clay-sand mixtures. Adv Mater Sci Eng 2013;2013. https://doi.org/10.1155/2013/562726.
[67] Tsubakihara Y, Kishida H, Nishiyama T. Friction between cohesive soils and steel. Soils Found 1993;33:145–56. https://doi.org/10.3208/SANDF1972.33.2_145.